Infrared photostimulation of the crista ampullaris

Suhrud M. Rajguru[1], Claus-Peter Richter[1,2,3], Agnella I. Matic[1], Gay R. Holstein[4], Stephen M. Highstein[5], Gregory M. Dittami[6] and Richard D. Rabbitt[5,6,7]

[1] *Department of Otolaryngology, Northwestern University, Chicago, IL 60611, USA*
[2] *Department of Biomedical Engineering, Northwestern University, Evanston, IL 60208, USA*
[3] *Hugh Knowles Center, Department of Communication Sciences and Disorders, Northwestern University, Evanston, IL 60208, USA*
[4] *Departments of Neurology and Neuroscience, Mount Sinai School of Medicine, New York, NY 10029, USA*
[5] *Marine Biological Laboratory, Woods Hole, MA 02543, USA*
[6] *Department of Bioengineering, University of Utah, Salt Lake City, UT 84112, USA*
[7] *Otolaryngology, Head & Neck Surgery, University of Utah, Salt Lake City, UT 84112, USA*

Non-technical summary It has been shown previously that application of short pulses of optical energy at infrared wavelengths can evoke action potentials in neurons and mechanical contraction in cardiac muscle cells. Optical stimuli are particularly attractive because of the ability to deliver focused energy through tissue without physical contact or electrical charge injection. Here we demonstrate efficacy of pulsed infrared radiation to stimulate balance organs of the inner ear, specifically to modulate the pattern of neural signals transmitted from the angular motion sensing semicircular canals to the brain. The ability to control action potentials demonstrates the potential of pulsed optical stimuli for basic science investigations and future therapeutic applications.

Abstract The present results show that the semicircular canal crista ampullaris of the toadfish, *Opsanus tau,* is sensitive to infrared radiation (IR) applied *in vivo.* IR pulse trains (~1862 nm, ~200 μs pulse^{-1}) delivered to the sensory epithelium by an optical fibre evoked profound changes in phasic and tonic discharge rates of postsynaptic afferent neurons. Phasic afferent responses to pulsed IR occurred with a latency of <8 ms while tonic responses developed with a time constant (τ) of 7 ms to 10 s following the onset or cessation of the radiation. Afferents responded to direct optical radiation of the sensory epithelium but did not respond to thermal stimuli that generated nearly equivalent temperature increases of the whole organ. A subset of afferent neurons fired an action potential in response to each IR pulse delivered to the sensory epithelium, at phase-locked rates up to 96 pulses per second. The latency between IR pulses and afferent nerve action potentials was much greater than synaptic delay and spike generation, demonstrating the presence of a signalling delay interposed between the IR pulse and the action potential. The same IR stimulus applied to afferent nerve axons failed to evoke responses of similar magnitude and failed to phase-lock afferent nerve action potentials. The present data support the hypothesis that pulsed IR activates sensory hair cells, thus leading to modulation of synaptic transmission and afferent nerve discharge reported here.

(Received 30 August 2010; accepted after revision 11 January 2011; first published online 17 January 2011)
Corresponding author S. M. Rajguru: 303 E Chicago Ave, 12-561 Searle, Chicago, IL 60611, USA.
Email: s-rajguru@northwestern.edu

Abbreviation AC, anterior canal; CC, common crus; EVS, efferent vestibular nucleus; IR, infrared radiation; LC, lateral canal; IP_3R, inositol trisphosphate receptor; mCU, mitochondrial calcium uniporter; mNCX, mitochondrial sodium/calcium exchanger; RyR, ryanodine receptor.

S. M. Rajguru and R. D. Rabbitt contributed equally to this work.

DOI: 10.1113/jphysiol.2010.198333

Introduction

Pulsed infrared radiation (IR, ∼1860 nm) and near infrared radiation (NIR, ∼790–850 nm) have been shown previously to elicit action potentials in sciatic (Wells *et al.* 2005), facial (Teudt *et al.* 2007) and auditory nerves (Izzo *et al.* 2006; Rajguru *et al.* 2010), as well as in pyramidal neurons (Hirase *et al.* 2002) and cardiomyocytes (Tseeb *et al.* 2009; Dittami *et al.* 2011). Recently stimulation at 1.875 μm has also been demonstrated to pulse lock the rate of intact embryonic quail hearts *in vivo* (Jenkins *et al.* 2010). Although the mechanism of action remains a topic of investigation and may vary between cell types, previous studies consistently report that IR applied to the cell body modulates intracellular $[Ca^{2+}]$ and that this signalling plays a major role in somatic IR excitability (Iwanaga *et al.* 2006; Smith *et al.* 2006; Smith *et al.* 2008). Evidence in cardiomyocytes suggests that 1862 nm pulsed IR activates the mitochondrial Ca^{2+} uniporter (mCU) and the mitochondrial Na^{+}/Ca^{2+} exchanger (mNCX) (Dittami *et al.* 2011). If IR-modulated $[Ca^{2+}]$ signalling is a general principle, we would expect inner-ear hair-cell organs to be sensitive to IR due to their high mitochondrial density and the $[Ca^{2+}]$-dependent synaptic machinery. To test IR photosensitivity, we applied 1862 nm, pulsed IR to the horizontal semicircular canal sensory epithelium of the toadfish *in vivo* using an optical fibre and recorded single-unit postsynaptic afferent nerve responses (Fig. 1). Direct comparisons were made between responses to IR, physiological mechanical stimulation, and electrical stimulation of the brainstem efferent vestibular nucleus. We also examined response sensitivity to whole-organ changes in temperature in the absence of direct IR stimulation of hair cells. Afferent responses to IR stimulation of the sensory epithelium were rapid and robust, and could not be reproduced by modulation of whole-organ temperature or efferent activation.

Methods

The use of adult oyster toadfish, *Opsanus tau,* of either sex, ∼500 g, was approved by the Institutional Animal Care and Use Committee at the Marine Biological Laboratory, MA. The experiments comply with the policies and regulations of *The Journal of Physiology* (Drummond, 2009). The toadfish is a well-established animal model for the vestibular physiology (Boyle & Highstein, 1990*b*; Rabbitt *et al.* 1995; Highstein *et al.* 1996) and was selected to facilitate experiments involving simultaneous mechanical stimulation, IR stimulation, efferent activation, and single unit afferent recordings *in vivo*. Physiological preparation, mechanical indentation and neural recordings followed methods described previously (Boyle & Highstein, 1990*a*; Boyle *et al.* 1991; Rabbitt *et al.* 1995; Highstein *et al.* 1996; Holstein *et al.* 2004*b*). Briefly, fish were anaesthetized with MS222 (3-aminobenzoic acid ethyl ester; Sigma; 25 mg ml^{-1} in seawater), partially immobilized through intramuscular injection of pancuronium bromide (0.05 mg kg^{-1}) in the tail, and secured in an experimental tank with two-thirds of its body and gills immersed in bubbled seawater (Instant Ocean, at 10–15°C). The eyes and remainder of the body were covered with moist tissue papers. A small craniotomy (3–4 mM in diameter) was performed lateral to the dorsal course of the anterior canal (AC) and rostral to the common crus (CC) to expose the lateral canal (LC) and nerve. This surgical approach allowed direct access to the LC nerve without disturbing the membranous labyrinth structures. During surgery, the perilymph within the upper region of the cavity was replaced with fluorocarbon (FC-75, 3M) to improve optical access to the nerve and canal structures, and to prevent tissue dehydration during the experimental procedure while maintaining normal afferent responses and canal biophysics (Rajguru & Rabbitt, 2007; Boyle *et al.* 2009; Rabbitt *et al.* 2009). Conventional glass microelectrodes were used for extracellular or intra-axonal afferent nerve recordings from the LC nerve about 1 mM from the ampulla. The extracellular potentials were conventionally amplified, filtered at 5 kHz, digitized at 10 kHz (ITC-18, HEKA Instrutech), and stored for subsequent analysis. Afferent responses were characterized in each animal using sinusoidal mechanical indentation (simulating head rotation) before, during, and after IR applied to the crista. Mechanical indentation of the semicircular canal limb used a 1.2 mm diameter glass rod attached to a closed-loop piezo-actuator and servo controller (P-843.60, E-625.SR, Physik Instrumente GmbH, Karlsruhe, Germany). Indentation causes physiological endolymphatic volume displacements (Dickman & Correia, 1989; Rabbitt *et al.* 1995) and allowed characterization of afferents. A waveform generator (Sony/Tektronix AFG 320) provided input to the piezo-actuator to deliver mechanical stimuli. Mechanical indentations were restricted to $<10\,\mu$m (equivalent to ∼40 deg s^{-1} angular head rotation) (Rabbitt *et al.* 1995). Temperature of the sensory epithelium was measured using a fast response micro-thermistor (QTUT-14C3, Quality Thermistor, Inc., Boise, ID, USA) placed in direct contact with the base of the crista at the nerve exit from the ampulla (Fig. 1). The micro-thermistor was calibrated prior to each experiment using a water bath. Stimulation of the efferent vestibular nucleus used 100 Hz bipolar optically isolated electrodes following previous reports in this species (Boyle & Highstein, 1990*a*; Boyle *et al.* 2009).

Optical stimulation of hair cells was achieved using a Capella pulsed infrared laser (Lockheed-Martin Aculight, Bothell, WA, USA) operated at 1862 nm, with trains of single pulses at repetition rates between 1 and 200 pps.

The pulse width was varied between 200 and 750 μs. Output from the laser was coupled to a 200 or 400 μm diameter low-OH optical fibre (Ocean Optics, Dunedin, FL, USA) for transmission and delivery. The optical fibre was mounted to a micromanipulator and positioned above the membranous wall of the LC ampulla, approximately 300–500 μm above hair cells, irradiating most of the sensory epithelium. The trigger from the laser source was recorded using a data acquisition system, and the radiant energy and pulse width were recorded. Digital data acquisition (ITC-18, HEKA Instrutech; Igor Pro, WaveMetrics, Lake Oswego, OR, USA) was used to record neural responses, displacement of the mechanical indenter, trigger signal from the infrared laser and temperature.

Data analysis was performed off-line by using custom software (Igor Pro, WaveMetrics). The data presented are mean ± standard deviation unless noted otherwise. Changes in background firing rate and degree of regularity (coefficient of variation) were calculated. For sinusoidal mechanical stimuli, the first harmonic gain and phase were computed for five or more consecutive stimulus cycles by manually selecting portions of the record. Spike times were averaged relative to the stimulus trigger using 100 bins per cycle phase histograms. Results were inverted to yield the firing rate (spikes s^{-1}) as a function of phase in the cycle. Empty bins were ignored in the fitting procedure, and the average rate was constrained to be ≥ 0. The changes in the afferent gain and phase induced by IR were measured by comparing responses for combined mechanical and IR stimuli and for mechanical stimuli alone.

Results

Pulsed IR of the crista ampullaris modulates discharge of primary afferent neurons

Single-unit semicircular canal afferent responses were recorded from the LC branch of the 8th cranial nerve while providing pulsed IR to the sensory epithelium and/or mechanical stimulation of the membranous duct as illustrated in Fig. 1. Afferents ($n = 60$) were divided into three groups based on their responses to tonic IR stimulation: excitatory 'on' responses (Fig. 2*A*, $n = 18$), inhibitory 'off' responses (Fig. 2*B*, $n = 35$) and mixed responses (Fig. 2*C*, $n = 7$). For the excitatory example (Fig. 2*A*) the radiation energy was 228 μJ $pulse^{-1}$ at a pulse rate of 50 pulses per second (pps). The afferent discharge rate increased with a time constant of $\tau_e \approx 3.3$ s during the IR stimulus and recovered to the pre-stimulus rate after stimulation following a time course of $\tau_{er} \approx 3.9$ s (summary, Fig. 3). For the inhibitory example (Fig. 2*B*), the IR energy was 358 μJ $pulse^{-1}$ at 100 pps. The discharge rate decreased with a time constant of $\tau_i \approx 3.4$ s during the IR stimulation and recovered to the pre-stimulus level with $\tau_{ir} \approx 1.4$ s. Whether a unit was inhibited or excited with IR did not change as a function of pulse rate. Two examples showing 'mixed' responses are provided in Fig. 2*C*. Mixed responses could be described as an inhibitory response followed by a relatively slow excitatory response. In 71% of the mixed responses, excitation exceeded inhibition, and the afferent discharge rate exceeded its pre-stimulus level during tonic IR stimulation. The IR dose–response relationship was tested in several units and was approximately linear. One example inhibitory response is shown in Fig. 2*D* (same afferent unit as shown in Fig. 2*B*). In this case, the response changed in a sigmoidal fashion with the radiation energy, while at energies higher than 858 μJ the IR stimulation resulted in near complete inhibition of the afferent response (Fig. 2*D* and *E*).

Population results are summarized in Fig. 3 which provides the background discharge rate in the control condition (filled) and the change in discharge rate re: control with tonic IR (Δ) (Fig. 3*A*); discharge regularity in the control condition (filled) and the change in regularity re: control (Δ) (Fig. 3*B*); and time constants for the change in discharge rate at the onset of IR (filled) and the cessation of IR (open) (Fig. 3*C*). $\Delta = 0$ corresponds to no change with IR relative to controls.

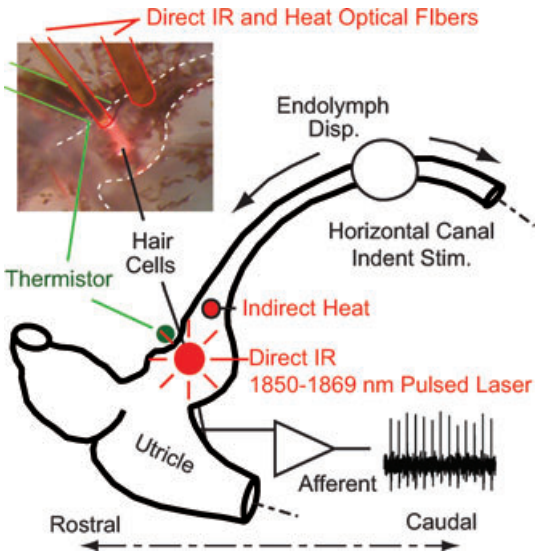

Figure 1. Experimental set-up
The lateral semicircular canal (LC) was stimulated by sinusoidal or step mechanical indentation of the membranous duct to induce controlled volumetric displacements of the cupula. IR (~1862 nm) was directly applied to the LC sensory epithelium to stimulate hair cells (inset, red pilot light) using a 200 or 400 μm diameter optical fibre near the outside surface of the ampulla. Whole-organ heat was applied using a second optical fibre located medial to the crista directing IR to the endolymph. Temperature was monitored using a micro-thermistor in contact with the base of the crista. Glass microelectrodes were used to record single-unit afferent responses of the 8th nerve branch for mechanical stimulation, direct IR optical stimulation and heat stimulation.

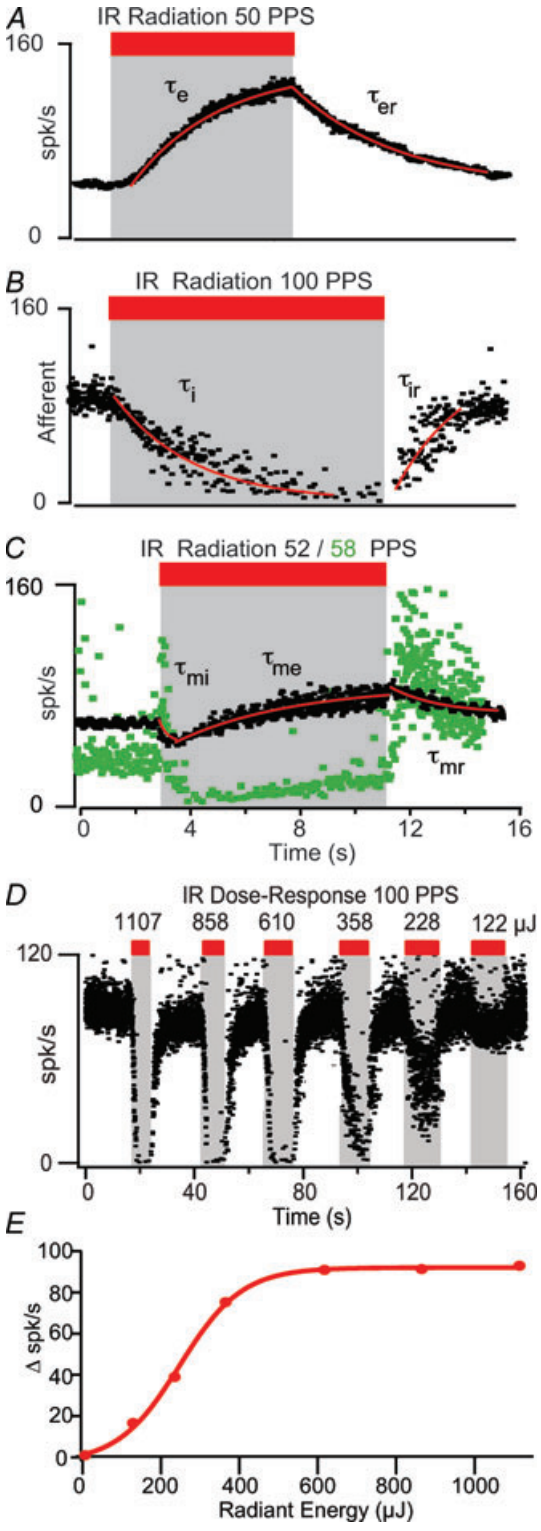

Figure 2. Sample records showing three types of responses to IR
A, excitatory 'on' ($n = 18$), *B*, inhibitory 'off' ($n = 35$), and *C*, mixed inhibitory-excitatory ($n = 7$). Exponential fits (red lines) illustrate the time course of afferent responses. *A*, an excitatory afferent, increased its firing rate from 63 spikes s^{-1} to 124 spikes s^{-1} in response to IR (50 pps, 228 μJ) with an onset time constant $\tau_e \approx 3.28$ s and recovered to pre-stimulus rate with time constant $\tau_{er} \approx 3.9$ s. *B*, inhibitory afferent, reduced its firing rate from 82 to 8 spikes s^{-1} in the presence of IR (100 pps, 358 μJ); onset time constant $\tau_i \approx 3.44$ s and recovery time constant $\tau_{ir} \sim 1.37$ s. *C*, mixed afferents, initial inhibition followed by excitation. In a subset of afferents excitation eventually exceeded inhibition leading to an increased discharge rate near the end of the stimulus (e.g. black, associated time constants were $\tau_{mi} \approx 0.29$ s, $\tau_{me} \approx 3.7$ s and $\tau_{mr} \approx 3.49$ s), while in other afferents inhibition dominated during IR but excitation dominated during the recovery period (e.g. green). *D* and *E*, example graded dose–response relationship from 122 to 1107 μJ $pulse^{-1}$ at 100 pps. The change in firing rate (i.e. the difference between the afferent's background firing rate and the firing rate with IR stimulation) with IR radiant energy per pulse is shown in *E*. For this afferent, the IR-induced change in firing rate occurred in a sigmoidal fashion with radiant energy (red curve).

Excitatory neurons ($n = 18$) increased their firing rate from an average of 59.9 spikes s^{-1} (±39.0 inter-afferent S.D.) in the control condition to 100.3 spikes s^{-1} (±52.8) with IR (mean energy ~750 μJ $pulse^{-1}$ at 60 pps). Three excitatory 'on' afferents were silent at rest, but fired at rates >50 spikes s^{-1} during IR stimulation of the sensory epithelium. The change (Δ) in discharge rate for individual 'on' afferents averaged 40.5 spikes s^{-1} (±39.0), a change from zero that was statistically significant ($^*P \leq 0.05$). Inhibitory 'off' neurons ($n = 35$) decreased their rate from 58 spikes s^{-1} (±36.6) at in the control condition to 14.7 spikes s^{-1} (±15.5) with IR (mean energy ~500 μJ $pulse^{-1}$ at 65 pps). The change in rate for 'off' afferents averaged −45.6 spikes s^{-1} (±38.0), a change from zero that was statistically significant ($^*P < 0.01$). Mixed response afferents ($n = 7$) initially decreased their rate from 73 spikes s^{-1} (±26.8 inter-afferent S.D.) in the control condition to 59.9 spikes s^{-1} (±31.0), and subsequently increased to 94.6 spikes s^{-1} (±49.0) with IR (mean energy 360 μJ $pulse^{-1}$ at 80 pps). These changes were also statistically significant. The coefficient of variation (CV) of the afferent discharge was higher for inhibitory afferents, relative to excitatory and mixed afferents (Fig. 3*B*). There were obvious changes in the CV in some units with IR stimulation (e.g. Fig. 2*C* green, note increased irregularity of interspike intervals at cessation of IR stimulus). Changes in afferent CV with tonic IR of the crista were statistically significant for all three types of units. This indicates that tonic IR likely affects transmitter release statistics since the CV is likely to be partially determined by statistics of transmitter release from hair cells.

Changes in discharge rate during tonic pulsed IR stimulation developed over time, following nearly exponential curves (Fig. 2, continuous red curves). The time constants for the population are well described by normal distributions and summarized in Fig. 3*C*. Two time constants are shown – one for the change in rate following the onset of tonic IR and the other for the recovery to baseline after cessation IR. Differences between

the average excitatory and inhibitory time constants were not statistically significant. The inhibitory time constant (τ_{mi}) for the mixed-type afferent was less than 1 s and significantly faster ($P < 0.05$) than other time constants.

Changes in whole-organ temperature cannot explain IR responses

The IR stimulus used in the present study is absorbed by the tissue and results in a temperature increase. To examine the potential role of changes in whole-organ temperature, we placed a micro-thermistor under the crista ampullaris. We monitored the changes in temperature while irradiating the sensory epithelium directly with IR and while delivering heat pulses to the endolymph using a second optical fibre at a location lateral to the crista (see Fig. 1). Figure 4 shows single unit afferent responses (black dots, left axis) and temperature (green curves, right axis). Note that the temperature measurements reported here are the whole-organ accumulated changes. IR evoked pulse-by-pulse temperature transients were not observed at the location of the thermistor, but might have been present in structures/organelles. Individual afferents responded robustly to direct IR of the sensory epithelium (Fig. 4*A* and *B*, left), but the same units showed almost no response to nearly identical temperature increases generated by heating of the endolymph and the entire crista ampullaris (Fig. 4*A* and *B*, right). Therefore, direct radiation of the sensory epithelium was required to elicit the responses summarized in Figs 2 and 3, and similar responses could not be evoked by heating the nerve bundle or by heating the organ through irradiating adjacent tissue. To further explore the role of temperature in evoked responses, we reduced the temperature of the entire fish by perfusing the tank with cooled seawater and repeating the IR experiments. Figure 4*C*–*E* provide examples from a cooled fish where the temperature was reduced from ∼23.5 to ∼17°C. At the lowest temperatures, the temperature-sensitive transient receptor potential cation channel TRPV1 would be expected to be inactivated. Responses were diverse, with amplitudes and time courses similar to those observed at normal room temperature, and generally did not correlate with whole-organ temperature. Note that IR responses were large even when the temperature increase caused by the radiation was <1°C and when the temperature increased remained well below room temperature. In Fig. 4*C* afferent discharge did correlate with temperature when the IR was off, but there was a substantial inhibitory effect of IR during radiation that did not correlate with temperature. Other afferents were excitatory during direct IR (Fig. 4*D*) and had inhibitory tails after cessation of IR the stimulus – responses that could not be explained by whole-organ temperature alone. Some of the most sensitive afferent neurons (Fig. 4*E*) fired an action potential for each IR pulse thus responding with a phase-locked band at the IR stimulus frequency (50 Hz in this example). Although rapid IR delivery and dispersion of heat pulses are likely to play a role in the responses (Olson *et al.* 1981*a*,*b*; Wells *et al.* 2007), the data in Fig. 4 clearly show that an IR-evoked change in whole-organ temperature is not responsible for the responses reported here. Rather, responses appear to be consistent with pulsed IR modulation of hair cell intracellular [Ca^{2+}]

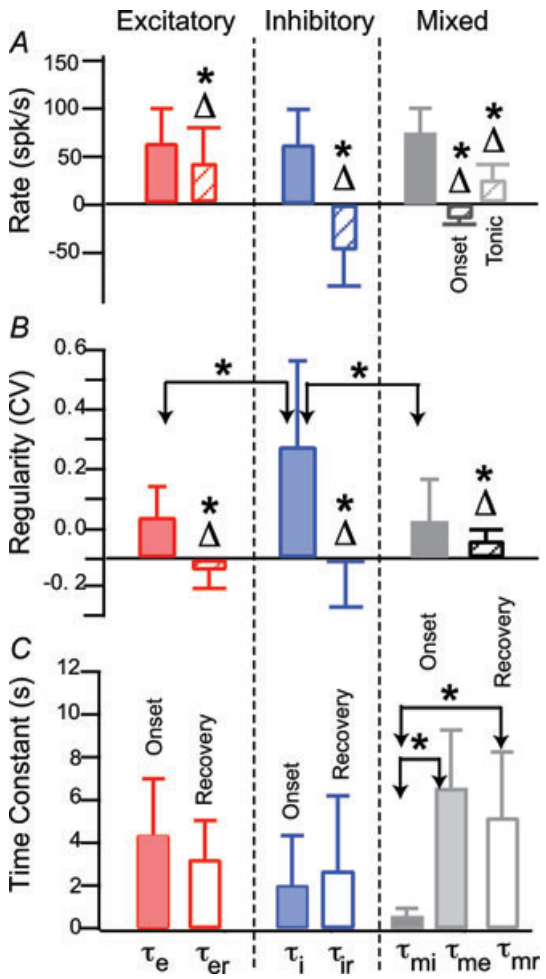

Figure 3. IR evoked change in afferent discharge rate, discharge regularity and time constants
A, afferent discharge rate in the control condition (filled) and the change in discharge evoked by tonic IR (Δ, hatched, difference between control and IR conditions) for excitatory (left column), inhibitory (centre column), and mixed units (right column). Error bars show inter-afferent standard deviation and reflect the endogenous diversity within the afferent population. *B*, regularity of afferent discharge rate (measured by the coefficient of variation, CV) in the control condition (filled) and the change in CV evoked by tonic IR (Δ, hatched, difference between control and IR conditions). *C*, exponential time constants measuring changes in afferent discharge at the onset of tonic IR, and recovery to the control condition after IR. Statistically significant differences between groups with $P < 0.05$ are indicated by * while statistically significant difference from zero for the changes evoked by IR ($P < 0.05$) are indicated by Δ*.

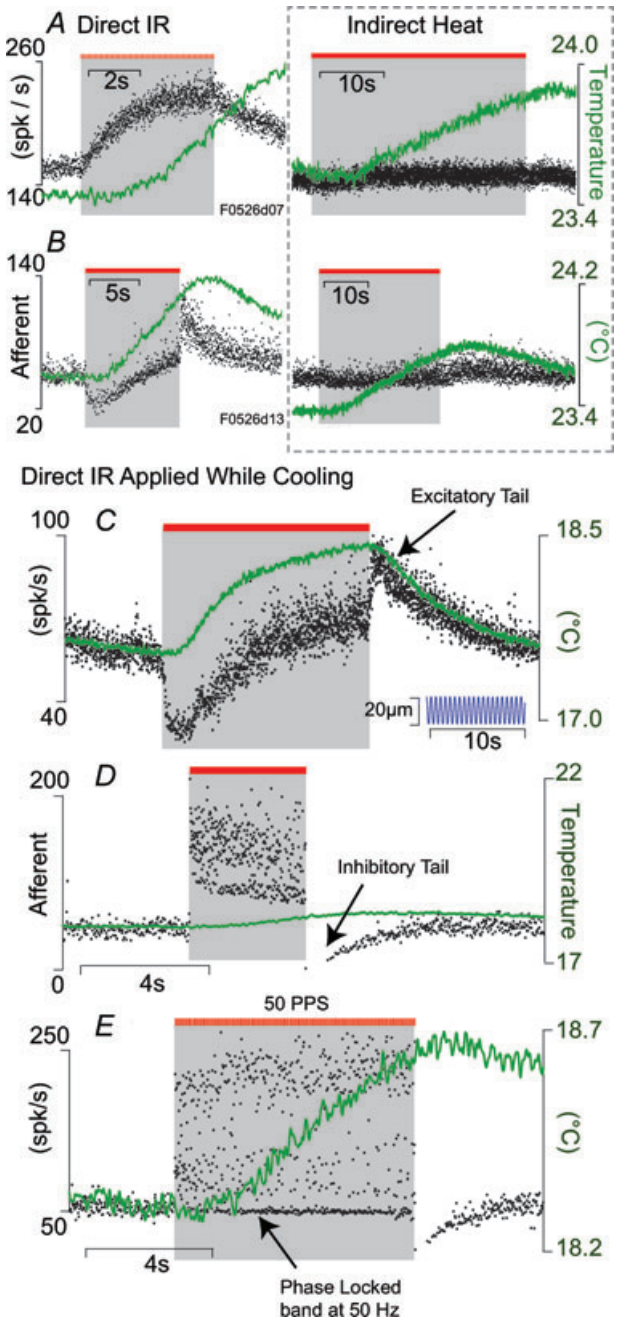

Figure 4. Afferent responses to direct IR of the sensory epithelium *vs.* indirect heat
A–B, single unit afferent responses (black dots, left axis) and whole-organ temperature (green, right axis) during direct IR of the sensory epithelium (left) and, for the same units, indirect heating of the organ (right). Responses to direct IR (left) were substantial while responses to similar temperature increases caused by indirect heat were very small (right). *C–E*, examples of direct IR stimulation of the sensory epithelium show a diverse relationship between afferent responses and whole organ temperature. Note, the fish was at room temperature in *A* and *B* (also Fig. 2) but cooled in *C–E* (right axis) to further demonstrate that IR-evoked responses are not simply the result of whole-organ temperature. For the afferent unit in *C*, sinusoidal mechanical indentation of the LC was on for the entire duration (inset).

and concomitant synaptic transmission, perhaps similar to IR-evoked responses reported previously in other cell types (Smith *et al.* 2008; Dittami *et al.* 2011).

Tonic pulsed IR stimulation modestly alters dynamic responses to physiological stimuli

We were interested in the extent to which tonic IR alters angular motion signal encoding. Afferent responses to sinusoidal mechanical stimuli are provided in Fig. 5 in the control condition and during tonic IR. In the present experimental model, the oyster toadfish, semicircular canal afferents encode angular head acceleration, angular velocity, or a mixture of the two (Boyle & Highstein, 1990*b*; Highstein *et al.* 2005). The sinusoidal mechanical stimulus used mimics sinusoidal angular head velocity. The unit in Fig. 5*A* responded with a maximum firing rate 46 deg phase (Fig. 5*A*, dashed grey line) advanced relative to peak mechanical stimulation at 2 Hz, and responded to tonic IR with a strong reduction in its background discharge rate and slightly reduced sensitivity to mechanical stimuli. There was also a small reduction in phase (<10 deg, Fig. 5*A*, dashed green line) during IR. More than 90% of afferents with a phase advance >45 deg (at 2 Hz) in the control condition were inhibited by infrared irradiation of the sensory epithelium. In contrast, the unit shown in Fig. 5*B* responded in phase with the mechanical stimulus and increased its background discharge rate with IR stimulation. Tonic IR also caused a small increase in sensitivity to mechanical stimuli – the gain increased from 20.4 to 24.9 spikes s^{-1} μm – but there was no significant change in the phase advance. Gain and phase results for IR excitatory 'on' afferents (left) and IR inhibitory 'off' afferents (right) are summarized in Fig. 5*C* in the form of Bode gain and phase (control: filled symbols; IR: open symbols). In general, the primary effect of tonic IR was on background discharge rate (Figs 1 and 4) – changes in sensitivity to physiological stimuli and mechanical displacements of hair bundles were present (Fig. 5), but less significant than changes in discharge rate.

Afferents phase-lock their discharge to the IR pulse train

About 15% of the afferents were tested for phase-locking and they responded with an action potential for each IR pulse. One-to-one phase-locked responses were observed for IR pulse rates from 10 to 96 pps. Figure 6*A* shows one example over a range of IR pulse frequencies (Fig. 6*A*: 10–33.7 pps), and a second example at 78 pps (Fig. 6*B–D*). The second afferent also phase-locked at other frequencies, both above and below its resting rate of 72 spikes s^{-1}. The inset (Fig. 6*E*) is a histogram showing the latency of action potentials relative to the IR pulse trigger. A Gaussian

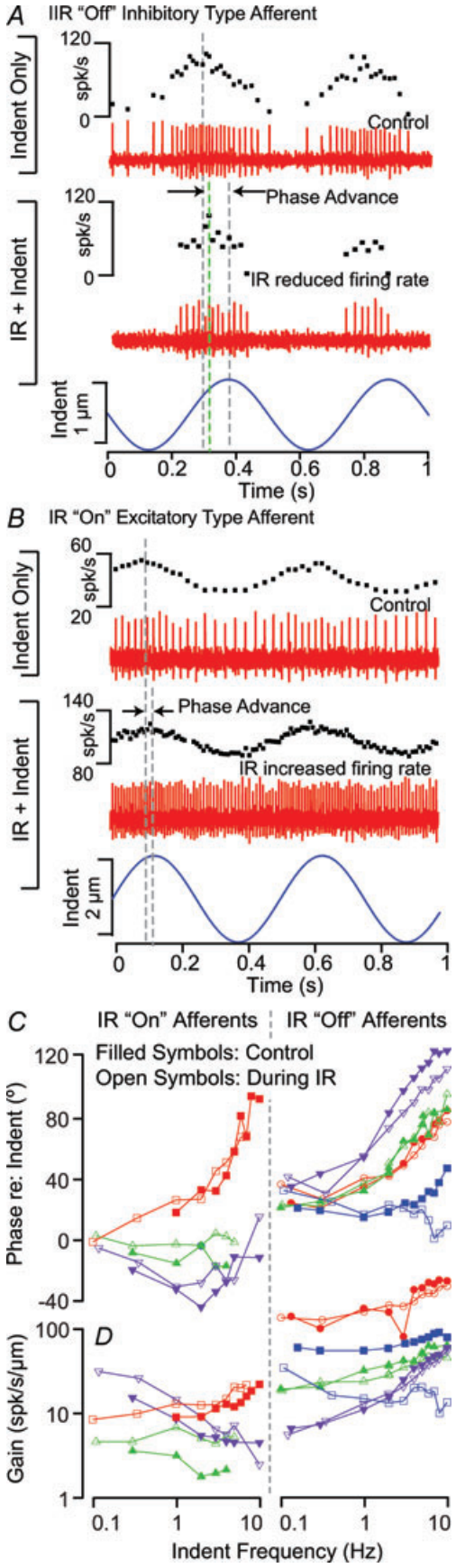

function was fitted to the histogram to find the latency (τ relative to the IR trigger). The mean latency over nine afferents tested was ~7.6 (±4.8) ms. This delay is significantly longer than synaptic delay for mechanical stimuli (0.6 ms, Rabbitt *et al.* 1995) and for trans-epithelial electrical stimulation (0.7 ms, Rabbitt *et al.* 1996) in the same species. This relatively long delay is consistent with the hypothesis that the IR action is primarily presynaptic and involves a hair-cell intracellular delay between the onset of irradiation and initiation of synaptic vesicle release. This relatively slow timing argues against the likelihood of direct photoactivated ionotropic depolarization of hair cells or afferent neurons, but supports the hypothesis of a photoactivated signalling mechanism (Smith *et al.* 2008; Tseeb *et al.* 2009; Dittami *et al.* 2011).

Mimicking responses to physiological stimuli

For the ~15% of primary afferents that were tested for phase locking with the IR stimulus pulse, a wide variety of afferent discharge patterns could be generated to mimic those evoked by physiological stimuli – providing the interspike interval was greater than ~10 ms. Some units exhibited phase locking with excellent dynamic range (e.g. Fig. 6). Others phase locked only over a limited range. About eighty-five per cent of the units could not be modulated on a spike-by-spike basis and did not phase-lock. It was possible, however, to simulate low frequency physiological responses in non-phase-locking afferents using slow modulation of the IR stimulus. Figure 7 shows the response of an afferent (pre-stimulus discharge rate ~58 spikes s^{-1}) to the frequency-modulated IR stimulus. The baseline afferent rate increased slowly from 58 to 117 spikes s^{-1} with superimposed

Figure 5. Combined tonic IR and sinusoidal mechanical indentation stimuli
A, inhibitory 'off' afferent showing periodic modulation in the control condition in response to indent (0.3 μm, zero-to-peak, 2 Hz sinusoid), and during tonic IR stimulation showing continued periodic modulation accompanied by a decrease in the average discharge rate. *B*, excitatory 'on' type afferent showing sinusoidal modulation in the control condition (0.5 μm, zero-to-peak, 2 Hz, sinusoidal indentation), and during tonic IR showing continued modulation accompanied by an increase in the average discharge rate. *C* and *D*, afferent sensitivity to mechanical stimuli in the form of Bode gain (spikes s^{-1} per μm mechanical indent) and phase (° relative to peak mechanical indent) as functions of frequency for 'on' (left) and 'off' (right) afferent neurons. Filled symbols show the control condition and open symbols show responses during tonic IR. Inhibitory 'off' type afferents generally were more phase advanced, and had a higher gain and more irregular discharge patterns than excitatory 'on' type afferents. IR-evoked changes in sensitivity to mechanical stimuli were small relative to the large changes in background discharge rate.

modulations due to changes in the IR stimulus frequency that generated discharge patterns similar to the control mechanical stimuli. Insets show nearly sinusoidal discharge modulations in response to IR.

IR stimulation of afferent nerve axons

Separate experiments revealed that direct IR applied to afferent nerve axons was much less efficacious than the same stimulus applied to the sensory epithelium. Figure 8*A* shows one of the more responsive afferent neurons, which slowly increased its discharge during IR stimulation of the nerve bundle. Results are summarized in Fig. 8*B* and *C*. Axonal IR stimulation increased the discharge rate in seven, decreased the rate in two, and had no detectable effect in 13 units. The time course of the responses due to direct IR stimulation of afferent

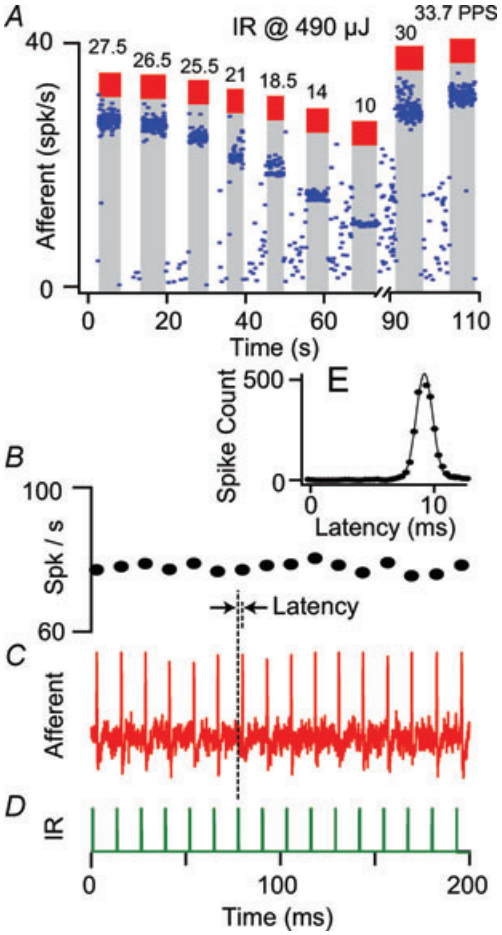

Figure 6. Afferents phase-locked to IR pulse trains (n = 9)
A, an example of phase locking of afferent discharge at various IR pulse train frequencies (10–33.7 pps). This particular afferent was nearly silent at rest. *B–D*, a second example showing phase locking at ~78 spikes s^{-1} in response to 200 μs-long, 610 μJ $pulse^{-1}$, IR pulses at 78 pps (*D*) (resting discharge rate: ~72 spikes s^{-1}, CV = 0.24). *E*, stimulus triggered histogram showing ~8.8 ms average latency of afferent discharge relative to the IR pulse.

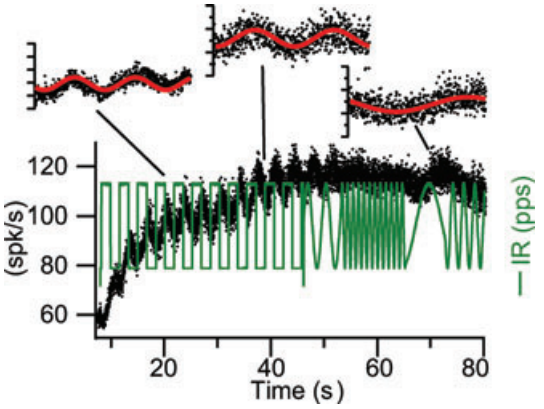

Figure 7. IR pulses applied to mimic neural responses produced by physiological stimuli
The rate of the IR was controlled to modulate transmitter release by hair cells and modulate afferent discharge. The excitatory type afferent (compare with Fig. 2) showed a slow increase in discharge rate accompanied by nearly sinusoidal response evoked by the IR (pulse per second) modulation.

axons was significantly slower than stimulation of the sensory epithelium (14.7 ± 11.4 s *vs.* 4.4 ± 2.6 s; cf. Figs 3 and 8), and we were not able to elicit phase locked responses in any units tested. The slower time course and weaker sensitivity of afferent axonal IR stimulation *vs.* crista ampullaris IR stimulation further supports the hypothesis that the primary action of pulsed IR applied

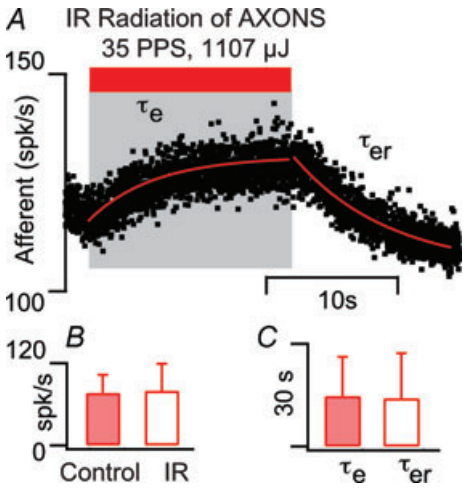

Figure 8. IR stimulation of afferent nerve axons (n = 22)
A, typical example showing modest increase in discharge rate from 120 spikes s^{-1} at rest to 129 spikes s^{-1} with IR stimulation. *B*, summary of discharge rate in the control condition (filled bars) and during tonic IR of nerve axons (open bars). We were unable to detect any change in discharge for axonal stimulation in over 50% of the units tested (n = 22). *C*, the excitation time constant for axonal IR stimulation was 14.7 ± 11.44 s (filled bars) compared to 4.35 ± 2.6 s sensory epithelium IR stimulation, and the recovery time constant was 14.11 ± 13.16 s (open bars) compared to 3.22 ± 1.8 s for sensory epithelium IR stimulation.

to the crista is to modulate structures specific to the end organ including sensory hair cells. Results also suggest there may be different mechanisms responsible for pulsed IR sensitivity in axons *vs.* cell bodies or synaptic terminals.

IR- *vs.* efferent-evoked afferent nerve responses

Afferent nerve sensitivity and firing rate are controlled through extensive efferent synaptic contacts on hair cells and afferents in the toadfish crista (Boyle & Highstein, 1990*a*; Boyle *et al.* 1991, 2009). To examine the possibility that IR might have modulated efferent synaptic inputs to hair cells or afferents we recorded single-unit afferent responses to bi-polar electrical stimulation of the brainstem efferent vestibular nucleus (EVS) and to IR stimulation of the crista. Figure 9 shows typical afferent responses. In Fig. 9*A*, notice the rapid increase in discharge rate during EVS followed by a slow adaptation back toward the resting rate (labelled *a*). This particular unit could not be inhibited by EVS and, in contrast, showed a rapid inhibition (labelled *b*) followed by a slow excitation for IR stimuli (labelled *c*). The variance of the inter-spike interval (*c*, CV) increased substantially during IR but did not change significantly during EVS. Figure 9*B* shows a second unit that did not respond to EVS but responded robustly to IR (labelled *d*). The periodic modulation in discharge was due to 2 Hz sinusoidal mechanical stimulation. Sensitivity of the neuron to mechanical stimulation (peak-to-peak modulation) slowly increased during IR and rapidly recovered to the control modulation at cessation of the IR stimulus (labelled *e*). In contrast to IR, EVS often reduces the sensitivity of afferents to mechanical stimulation due to inhibitory synaptic contacts on hair cells (Boyle *et al.* 2009), but EVS has never been observed to increase the sensitivity as shown here for IR. Figure 9*C* shows a third unit that was inhibited by IR (labelled *f*) but showed almost no change in discharge to EVS (labelled *h*). The slow modulation (labelled *g*) is a respiration movement artifact present in this animal that was eliminated with EVS (labelled *h*), consistent with previous reports in this species and confirming EVS effectively activated the vestibular nucleus (Highstein & Politoff, 1978). Additional afferent records showing EVS modulation were obtained without changing any parameters both before and after the examples shown in Fig. 9. These data demonstrate that the major origin of IR sensitivity is not activation of the efferent system.

Discussion

Present results show that the semicircular canal vestibular neuroepithelium is highly sensitive to 1862 nm pulsed IR stimulation (Figs 2 and 6). Diverse inhibitory 'off' and excitatory 'on' afferent responses were observed. Afferent responses were absent, or substantially smaller, when IR was applied to afferent nerve axons (Fig. 8), or when heat was applied to the sensory epithelium without direct radiation of the crista ampullaris (Fig. 4). Some afferent neurons fired an action potential in response to each IR pulse following a latency of ~7.6 ms (Fig. 6). Further, the afferent responses cannot be explained by activation of the efferent vestibular system (Fig. 9). Together, these data show that the IR responses cannot be explained by direct activation of afferent neurons, modulation of efferent synaptic inputs, or whole-organ temperature changes. Direct radiation was required, thus suggesting IR photosensitivity was a local event distinct from global changes in temperature. Given the present data, it is likely that IR acted primarily on hair cells to evoke changes in synaptic transmission to afferent neurons. Diversity of IR responses indicates the stimulus might have multiple sites of action, some of which are discussed below.

In other excitable cells studied to date, pulsed IR applied to the soma evokes intracellular [Ca^{2+}] transients that appear to be fundamental to IR photosensitivity (Smith *et al.* 2006, 2008; Dittami *et al.* 2011). The

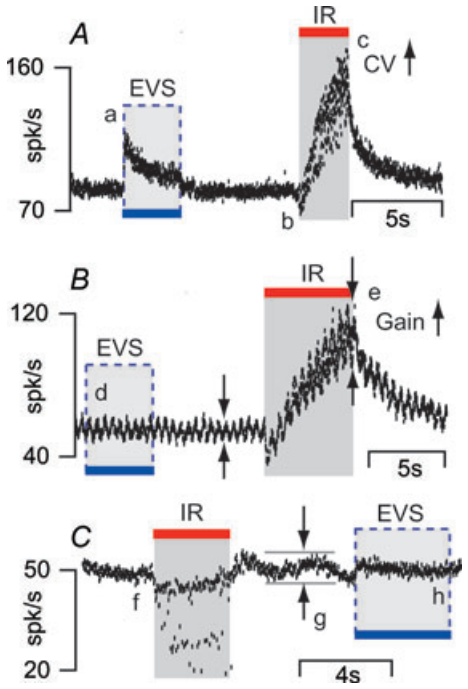

Figure 9 IR- *vs.* efferent-evoked afferent responses
Responses of three different afferents to separate IR and efferent vestibular stimulation (EVS) are shown. *A*, one unit showed an excitatory response (*a*) to EVS followed by a slow adaptation to resting discharge rate. The same unit elicited a mixed-type response to IR. Unlike EVS, IR evoked a rapid inhibitory response (*b*) followed by excitation (*c*) and increased the variance of interspike interval (CV) of the afferent unit. *B*, a second afferentunit did not respond to EVS (*d*) but elicited a strong response to IR (discharge rate increased from ~50 spikes s^{-1} to ~100 spikes s^{-1}, e). *C*, a third unitwas inhibited by IR (f) but did not respond to EVS. EVS did eliminate (*h*) the respiratory motion artifact (*g*) from the afferent response.

mechanism(s) underlying [Ca^{2+}] transients may vary between cell types and stimulus parameters, but the transients suggest some common mechanisms. When the identical 1862 nm pulsed IR stimulus used in the present study was applied to neonatal cardiomyocytes, pharmacological and [Ca^{2+}] imaging evidence indicated IR activated mitochondrial mNCX and mCU Ca^{2+} transport (Dittami *et al.* 2011). mCU was rapidly activated by IR to induce Ca^{2+} influx (acting as a fast cytosolic Ca^{2+} buffer) while mNCX was activated to induce Ca^{2+} efflux on a slower time scale. In cardiomyocytes, IR photoactivated fluxes modulated cytosolic [Ca^{2+}] and entrained large ryanodine receptor (RyR) mediated Ca^{2+}-activated Ca^{2+} transients. Additional evidence also implicates a role for inositol trisphosphate receptors (IP_3R) in IR/heat-pulse [Ca^{2+}] responses (Tseeb *et al.* 2009; Dittami *et al.* 2011). Precisely why mitochondrial excitation occurred in previous studies is not known, but one hypothesis could be that a mitochondrial chromophore is responsible for IR optical absorption thus leading to rapid thermal transients localized to mitochondria (Salet *et al.* 1979; Szundi *et al.* 2001). If mitochondrial activation was a factor in the present study, radiation of the crista would have delivered energy to mitochondria in hair cells, afferent nerve terminals and efferent nerve terminals (Sans & Highstein, 1984; Sato *et al.* 1988). Present data are not sufficient to rule out any of these possibilities, but recordings during efferent stimulation (Fig. 9) indicate that any IR action on efferent inputs to hair cells or afferents was likely to be small relative to other factors. This implies that primarily hair cells and/or afferent nerve endings are sensitive to IR.

Consistent with action primarily on hair cells, a recent study (Feng *et al.* 2010) reported an increase in inhibitory postsynaptic currents with presynaptic pulsed IR stimulation in rat cortical neurons. The present data are consistent with these previous data and with the hypothesis that pulsed IR modulated intracellular [Ca^{2+}] in presynaptic sensory hair cells and, following a signalling delay, modulated synaptic transmission to afferent neurons. In this hypothetical model, the ∼7.6 ms latency between the optical pulse and the afferent nerve response would be attributed to intracellular hair cell Ca^{2+} signalling. Further supporting this idea, synaptic delay in the toadfish has been reported to be ∼0.6 ms (Rabbitt *et al.* 1995), which is much shorter than the latency observed with IR. An optoacoustic effect gating cation channels or the mechano-electrical transduction channels in the hair cells would be expected to approach this synaptic delay with increased IR intensity. In the phase locked units, the latency to IR stimuli did not reduce with increasing IR intensity, which rules out such an optoacoustic effect and suggests a chemical signalling delay. Also, some afferent units that phase locked to the mechanical stimuli could not be phase locked to the IR stimuli. Conversely, in other units that phase locked to IR, it was not possible to evoke phase locking to mechanical stimuli. This difference also argues against any opto-mechano-transduction mechanism.

The absence of robust afferent responses to whole organ temperature increases and persistence of IR-evoked responses, even after the animal's temperature was reduced by 6–7°C, rules out a simple equilibrium thermodynamic origin. The low temperature would also be expected to inactivate TRPV channels. Instead of an accumulated temperature change, the responses of the primary afferents to IR apparently are governed by transient, pulse-by-pulse optical energy. Although evidence noted above suggests intracellular origins, the dynamic also raises the possibility that heat pulses might have led to thermal expansion of the tissue. It is not clear if differential expansion of water *vs.* membrane and integral proteins would lead to stretch activation of ion channels, or if such channels exist in vestibular hair cells. Nonetheless, cation permeable channels have been reported in the lateral membrane of outer hair cells in the guinea pig cochlea (Ding *et al.* 1991; Iwasa *et al.* 1991; Zheng *et al.* 2003). It has been reported that these channels are activated by stretch and we cannot completely rule out their involvement in IR evoked response reported here. Irrespective of the specific mechanism(s), it is likely that 1862 nm IR applied to the semicircular canal crista ampullaris evoked [Ca^{2+}] transients in hair cells. If true, IR-evoked [Ca^{2+}] modulation would alter hair-cell synaptic transmission and might explain changes in postsynaptic afferent responses reported here.

The fact that both excitatory 'on' and inhibitory 'off' afferent IR responses were observed is significant. Inhibitory responses occurred preferentially in afferents that responded to sinusoidal mechanical indentation with a high degree of phase advance (Fig. 5*C*) and in units that exhibited more irregular spontaneous discharge patterns (Fig. 3*B*). Highly phase advanced afferent responses are not present in mammalian semicircular canals, and occur in the toadfish due to a convergence of excitatory inputs from glutamatergic hair cells and inhibitory inputs from GABAergic hair cells (Holstein *et al.* 2004*a*). In the vestibular system, individual afferents are postsynaptic to multiple sensory hair cells. Hence, the IR response of a specific afferent would be expected to depend upon the particular synaptic organization, transmitter-type of its synaptic inputs and the extent to which various hair cell types are activated by IR. There is currently no evidence of GABAergic hair cells in the mammalian crista. Therefore it is possible that inhibitory 'off' type IR responses might not be as pronounced in mammals.

Inconsistent with the GABA-mediated inhibitory 'off' type response correlate, we recorded responses of a few afferent neurons that exhibited IR-evoked 'off' responses but did not contact GABAergic hair cells (as evidenced by a lack of phase advance at 2 Hz; Holstein *et al.* 2004*a*). Although these neurons were exceptions in the present

toadfish experiments, representing <10% of neurons recorded, they might be more prevalent in mammals and therefore important for future applications of IR stimuli. It is possible that IR 'off' responses might have involved a reduction in the release of glutamate. As discussed above, IR mitochondrial activation might have caused a rapid decrease in cytosolic $[Ca^{2+}]$, perhaps followed by an increase. The relative magnitudes or even existence of these two transients is not known in hair cells, nor are the spatial distributions of $[Ca^{2+}]$ microdomains evoked by IR. It might also be of importance that outward Ca^{2+}-activated K^+ channels are found in auditory inner hair cells. An IR led increase in intracellular $[Ca^{2+}]$ could activate K^+ channels, hyperpolarize some of the hair cells and reduce the modulation of postsynaptic afferent neurons in response to mechanical inputs. This may explain the observations of inhibitory and/or mixed type afferent responses observed in the present study.

The present work is focused on afferent responses evoked from infrared irradiation of the crista. It is important to note that the present results do not directly support or refute the involvement of intracellular Ca^{2+}. Although combined with data from other studies, results are consistent with the hypothesis that 1862 nm pulsed IR modulated intracellular $[Ca^{2+}]$ in hair cells and/or postsynaptic afferent terminals and that this was the primary signal leading to changes in synaptic transmission and postsynaptic afferent discharge. Results indicate that pulsed IR may prove useful to modulate excitability of various cell types through manipulation of Ca^{2+} signalling.

References

Boyle R, Carey JP & Highstein SM (1991). Morphological correlates of response dynamics and efferent stimulation in horizontal semicircular canal afferents of the toadfish, *Opsanus tau*. *J Neurophysiol* **66**, 1504–1521.

Boyle R & Highstein SM (1990*a*). Efferent vestibular system in the toadfish: action upon horizontal semicircular canal afferents. *J Neurosci* **10**, 1570–1582.

Boyle R & Highstein SM (1990*b*). Resting discharge and response dynamics of horizontal semicircular canal afferents of the toadfish, *Opsanus tau*. *J Neurosci* **10**, 1557–1569.

Boyle R, Rabbitt RD & Highstein SM (2009). Efferent control of hair cell and afferent responses in the semicircular canals. *J Neurophysiol* **102**, 1513–1525.

Dickman JD & Correia MJ (1989). Responses of pigeon horizontal semicircular canal afferent fibers. I. Step, trapezoid, and low-frequency sinusoid mechanical and rotational stimulation. *J Neurophysiol* **62**, 1090–1101.

Ding JP, Salvi RJ & Sachs F (1991). Stretch-activated ion channels in guinea pig outer hair cells. *Hear Res* **56**, 19–28.

Dittami GM, Rajguru SM, Lasher R, Hitchcock R & Rabbitt RD (2011). Intracellular calcium transients evoked by pulsed infrared radiation in neonatal cardiomyocytes. *J Physiol* **589**, 1295–1306.

Drummond GB (2009). Reporting ethical matters in *The Journal of Physiology*: standards and advice. *J Physiol* **587**, 713–719.

Feng HJ, Kao C, Gallagher MJ, Jansen ED, Mahadevan-Jansen A, Konrad PE & Macdonald RL (2010). Alteration of GABAergic neurotransmission by pulsed infrared laser stimulation. *J Neurosci Methods* **192**, 110–114.

Highstein SM & Politoff AL (1978). Relation of interspike baseline activity to the spontaneous discharges of primary afferents from the labyrinth of the toadfish, *Opsanus tau*. *Brain Res* **150**, 182–187.

Highstein SM, Rabbitt RD & Boyle R (1996). Determinants of semicircular canal afferent response dynamics in the toadfish, *Opsanus tau*. *J Neurophysiol* **75**, 575–596.

Highstein SM, Rabbitt RD, Holstein GR & Boyle RD (2005). Determinants of spatial and temporal coding by semicircular canal afferents. *J Neurophysiol* **93**, 2359–2370.

Hirase H, Nikolenko V, Goldberg JH & Yuste R (2002). Multiphoton stimulation of neurons. *J Neurobiol* **51**, 237–247.

Holstein GR, Martinelli GP, Boyle R, Rabbitt RD & Highstein SM (2004*a*). Ultrastructural observations of efferent terminals in the crista ampullaris of the toadfish, *Opsanus tau*. *Exp Brain Res* **155**, 265–273.

Holstein GR, Rabbitt RD, Martinelli GP, Friedrich VL Jr, Boyle RD & Highstein SM (2004*b*). Convergence of excitatory and inhibitory hair cell transmitters shapes vestibular afferent responses. *Proc Natl Acad Sci U S A* **101**, 15766–15771.

Iwanaga S, Kaneko T, Fujita K, Smith N, Nakamura O, Takamatsu T & Kawata S (2006). Location-dependent photogeneration of calcium waves in HeLa cells. *Cell Biochem Biophys* **45**, 167–176.

Iwasa KH, Li MX, Jia M & Kachar B (1991). Stretch sensitivity of the lateral wall of the auditory outer hair cell from the guinea pig. *Neurosci Lett* **133**, 171–174.

Izzo AD, Richter C-P, Jansen ED, Joseph T & Walsh J (2006). Laser stimulation of the auditory nerve. *Laser Surg Med* **38**, 745–753.

Jenkins MW, Duke AR, Doughman Y, Chiel HJ, Fujioka H, Watanabe M, Jansen ED & Rollins AM (2010). Optical pacing of the embryonic heart. *Nat Photonics* **4**, 623–626.

Olson JE, Schimmerling W, Gundy GC & Tobias CA (1981*a*). Laser microirradiation of cerebellar neurons in culture. Electrophysiological and morphological effects. *Cell Biophys* **3**, 349–371.

Olson JE, Schimmerling W & Tobias CA (1981*b*). Laser action spectrum of reduced excitability in nerve cells. *Brain Res* **204**, 436–440.

Rabbitt RD, Boyle R & Highstein SM (1995). Mechanical indentation of the vestibular labyrinth and its relationship to head rotation in the toadfish, *Opsanus tau*. *J Neurophysiol* **73**, 2237–2260.

Rabbitt RD, Breneman KD, King C, Yamauchi AM, Boyle R & Highstein SM (2009). Dynamic displacement of normal and detached semicircular canal cupula. *J Assoc Res Otolaryngol* **10**, 497–509.

Rabbitt RD, Highstein SM & Boyle R (1996). Determinants of semicircular canal afferent response dynamics in fish. *Ann N Y Acad Sci* **781**, 213–243.

Rajguru SM, Matic AI, Robinson AM, Fishman AJ, Moreno LE, Bradley A, Vujanovic I, Breen J, Wells JD, Bendett M & Richter CP (2010). Optical cochlear implants: Evaluation of surgical approach and laser parameters in cats. *Hear Res* **269**, 102–111.

Rajguru SM & Rabbitt RD (2007). Afferent responses during experimentally induced semicircular canalithiasis. *J Neurophysiol* **97**, 2355–2363.

Salet C, Moreno G & Vinzens F (1979). A study of beating frequency of a single myocardial cell. III. Laser micro-irradiation of mitochondria in the presence of KCN or ATP. *Exp Cell Res* **120**, 25–29.

Sans A & Highstein SM (1984). New ultrastructural features in the vestibular labyrinth of the toadfish, *Opsanus tau*. *Brain Res* **308**, 191–195.

Sato F, Sasaki H & Mannen H (1988). Electron microscopic comparison of the terminals of two electrophysiologically distinct types of primary vestibular afferent fibers in the cat. *Neurosci Lett* **89**, 7–12.

Smith NI, Iwanaga S, Beppu T, Fujita K, Nakamura O & Kawata S (2006). Photostimulation of two types of Ca^{2+} waves in rat pheochromocytoma PC12 cells by ultrashort pulsed near-infrared laser irradiation. *Laser Phys Lett* **3**, 154–161.

Smith NI, Kumamoto Y, Iwanaga S, Ando J, Fujita K & Kawata S (2008). A femtosecond laser pacemaker for heart muscle cells. *Optics Express* **16**, 8604–8616.

Szundi I, Liao G-L & Einarsdottir O (2001). Near-infrared time-resolved optical absorption studies of the reaction of fully reduced cytochrome c oxidase with dioxygen. *Biochemistry* **40**, 2332–2339.

Teudt IU, Nevel A, Izzo AD, Walsh J, JT & Richter C-P (2007). Optical stimulation of the facial nerve – a new monitoring technique? *Laryngoscope* **117**, 1641–1647.

Tseeb V, Suzuki M, Oyama K, Iwai K & Ishiwata S (2009). Highly thermosensitive Ca dynamics in a HeLa cell through IP_3 receptors. *HFSP J* **3**, 117–123.

Wells J, Kao C, Jansen ED, Konrad P & Mahadevan-Jansen A (2005). Application of infrared light for in vivo neural stimulation. *J Biomed Opt* **10**, 064003.

Wells J, Kao C, Konrad P, Milner TE, Kim J, Mahadevan-Jansen A & Jansen ED (2007). Biophysical mechanisms of transient optical stimulation of peripheral nerve. *Biophys J* **93**, 2567–2580.

Zheng J, Dai C, Steyger PS, Kim Y, Vass Z, Ren T & Nuttall AL (2003). Vanilloid receptors in hearing: altered cochlear sensitivity by vanilloids and expression of TRPV1 in the organ of corti. *J Neurophysiol* **90**, 444–455.

Author contributions

S.M.R., C.P.R., A.I.M., S.M.H., G.R.H., G.M.D. and R.D.R. designed and conducted experiments; S.M.R. and R.D.R. analysed the data and wrote the manuscript. All authors approved the final version of the manuscript.

Acknowledgements

Funding sources: NIH R01DC006685, R01DC004928 (R.D.R.) and R41DC008515 (C.P.R.).